Low Temperature Physics/Fizika Nizkikh Temperatur, 2021, vol. 47, No. 11, pp. 981–988

Local spin-triplet superconductivity in half-metallic manganites: A perspective platform for high-temperature topological superconductivity

V. N. Krivoruchko

Donetsk Institute for Physics and Engineering named after A. A. Galkin of the National Academy of Sciences of Ukraine
Kyiv 03028, Ukraine
E-mail: krivoruc@gmail.com

Received May 15, 2021, published online September 24, 2021

Topological materials and their unusual properties are nowadays a focus of experimental and theoretical research. Promising systems where topological superconducting phases can be realized are materials with a spin-triplet superconducting state. Yet, in the nature superconductors with a spin-triplet *p*-wave pairing are exceptions. The experimentally accessible way to overcome this bottleneck is spin-triplet pairing induced in proximitized structures of spin-singlet superconductors with time-reversal symmetry breaking counterparts. We discuss the possibility of creating such materials using superconductor–half-metallic manganite nanostructures. A unique promising feature of the proximity-coupled hybrid structures is high-temperature local triplet superconductivity in half-metallic manganites. The experimental evidence of a latent spin-triplet pairing in half-metallic manganites is presented and conditions favoring the topological superconducting state in nanostructures based on them are discussed.

Keywords: half-metallic manganites, localized superconducting Cooper pairs, topological superconductivity, superconductor–ferromagnet heterostructures.

"A promising ground for topological superconductivity is the spin-triplet … pairing state."
M. Sato, Y. Ando, *Topological superconductors: a review*,
Rep. Prog. Phys. **80**, 076501 (2017).

1. Introduction

Currently, in the condensed matter physics, a "second quantum revolution" is carried out through the introduction of topology-originated concepts used to characterize physical states and properties of solids. With the introduction of topology, the description of phase transitions and phases of the system expands, and includes not only transitions differentiating in terms of a local (Landau) order parameter, but also those characterized in terms of global quantities that are measured nonlocally and which endow the system with global stability to perturbations. The topological state is a state of matter characterized by nonzero topological number of the wave functions and nontrivial topological states of their quasiparticles. A typical example is a superconductivity. Topologically protected non-Abelian excitations in a superconducting state are equivalents of the Majorana fermions (MFs) — fundamental particles originally proposed in 1937 by E. Majorana as a real solution to the Dirac equation (an MF is a fermion that is its own antiparticle has no charge but can carry spin or heat). Topological superconducting states support topologically protected gapless Andreev bound states (ABSs) that are their own antiparticles, and which partially mimic the so-called zero mode MFs. Recently, a great effort has been put towards an unambiguous experimental detection of MFs in systems which, as expected, can be in the topological superconducting state (see, e.g., reviews [1–3] and references therein).

Though topological materials and their unusual properties are in the focus of modern experimental and theoretical research in condensed matter physics, beyond doubt experimental identification/observation of Majorana quasiparticles is still absent. Concerning the superconducting state, small proximity induced triplet energy gap, which implements the topological pairing gap Δ_{top}, and pair-breaking impurities local states, the so-called Yu–Shiba–Rusinov states (see, e.g., review [4]), which spoil the spectral resolution in experiments performed at sub-Kelvin temperatures, are

among primary reasons. The inability to distinguish experimentally whether the observed peculiarities are due to topological or non-topological (trivial/local) states blocks further progress in the subject.

Promising materials for the topological superconducting phase realization are materials with the spin-triplet superconducting pairing state [3]. Indeed, in a *p*-wave superconductor (SC) the Bogoliubov quasiparticles, $b_{\mathbf{k}\sigma} = u c_{\mathbf{k}\sigma} + v c_{-\mathbf{k}\sigma}^{+} = (u - v^{*}) c_{\mathbf{k}\sigma} + (v^{*} c_{\mathbf{k}\sigma} + v c_{-\mathbf{k}\sigma}^{+})$, have both electron and hole components of equal spin projection, σ, and thus can possess the MFs properties. The task is to create necessary conditions when *p*-wave Bogoliubov quasiparticles are "forced" to demonstrate their MFs characteristics, i.e., when $b_{\mathbf{k}\sigma} \to (v^{*} c_{\mathbf{k}\sigma} + v c_{-\mathbf{k}\sigma}^{+})$. Yet, SCs realizing a spin-triplet *p*-wave pairing are not common in nature; Sr_2RuO_4 with critical temperature $T_c \approx 1.5$ K being the only realistic candidate so far. A way that overcomes this difficulty settles in artificially engineered topological materials. Artificially engineered topological superconductivity in SC-magnet hybrid structures is currently attracting attention, because, as expected, they represent one of the most promising platforms for realizing topological superconducting phases [3, 5–9]. Particularly, Choy *et. al*. has proposed to create MFs by depositing a chain of magnetic nanoparticles on an *s*-wave superconducting substrate [5]. In this system, the transition into a topologically nontrivial phase is governed by two types of disorder: (i) a variation in the orientation of the magnetic moments on nearby nanoparticles needed to open a gap in the excitation spectrum — a prerequisite for a topological phase; and (ii) disorder in the hopping energies to localize a pair of weakly coupled MFs at the chain ends. Chung *et al.* [6] consider the creation of spin-triplet superconductivity and topological phase in SC/half-metal heterostructures (a half-metal is a spin-polarized metal at the Fermi surface, i.e., a metal for the majority spin and an insulator for the minority spin). The band computations performed for two atomic layers of VTe and CrO_2 showed that this type of heterostructures is a suitable candidate material.

In this report, we discuss a promising, in our opinion, way for creating artificial materials with a high-temperature topological superconductivity. These are hybrid spin-singlet superconductors–half-metallic manganites nanostructures; in particular, chains of half-metallic manganites nanoparticles on an *s*-wave SC substrate. A key factor of these hybrid structures is *local high-temperature triplet superconductivity* of half-metallic manganites. The experimental evidence for the existence of latent (noncoherent) spin-triplet pairing in half-metal manganites is presented and conditions favoring their topological superconductivity are discussed. The work is substantially based on the experimental results, especially obtained in Refs. 10–19, evidencing unconventional superconducting proximity effect in SC/half-metallic manganites hybrid structures.

2. Local superconductivity in a phase-fluctuating superconductor

According to the Bardeen–Cooper–Schrieffer (BCS) theory, the transition to the superconducting state is accompanied and is caused by a rearrangement of the electronic spectrum with the appearance of a gap at the Fermi level. The state is characterized by a complex order parameter (see, e.g., reviews [20–22]):

$$\Delta(\mathbf{r}) = \left|\Delta(\mathbf{r})\right| \exp\left\{\varphi(\mathbf{r})\right\},$$

where the modulus of the pairing energy, namely $2|\Delta(\mathbf{r})|$, is the gap value in the electronic spectrum. In the mean field theory, temperatures of the electron-pairing effect, T_Δ, and the long-range (global) phase coherency, $T\varphi$, coincide and yield the critical temperature, T_c. This silently implies that the spatial variations in $|\Delta(\mathbf{r})|$ are small, and that global phase coherence temperature $T\varphi$ is larger than (or equal to) T_c.

In a system with a small superfluid density (bad metals with an electron concentration that is substantially less than that characteristic of conventional metals) the spatial variations/fluctuations in the order parameter $\Delta(\mathbf{r})$, e.g., due to thermal effects, become crucial in the regions where pairing energy value $|\Delta(\mathbf{r})|$ is small. As the result, in a bad metal the thermal fluctuations in the global phase coherency of the order parameter are the most important ones. The fluctuations of the order parameter phase $\varphi(\mathbf{r})$ in mesoscopic "islands" prevent the long-range superconductivity. Therefore, for systems with low conductivity and small superfluid density, the temperature of the system's global phase coherency $T\varphi$ can be reduced significantly and could be smaller than the "islands" pairing temperature T_Δ. Then the sample's superconducting transition temperature T_c is determined by the global phase coherency, whereas the pair condensate could exist well above $T_c = T\varphi < T_\Delta$ [20–22].

An important consequence of the Cooper pairs fluctuation above the transition temperature T_c is the appearance of the so-called pseudo-gap [20–26], i.e., a reduction of the single-electron density of states near the Fermi level. According to the viewpoint expressed in [23], the pseudo-gap state in high-T_c cuprates could be considered as an unconventional metal, i.e., as a SC that has lost its phase stiffness due to phase fluctuations. Doped manganites are bad metals, and a large pseudo-gap is detected in numerous experiments on manganites [27–30]. It may be suggested that at least a part of the observed pseudo-gap value is due to pairing without the global phase coherency. In cuprates, an additional argument for the local pair's condensate existence at $T > T_c$ is a diamagnetism observed just above T_c, i.e., when temperature $T\varphi < T < T_\Delta$ (see, e.g., Refs. 31 and 32). For manganites, however, this kind of the superfluid density precursor can be strongly suppressed by a ferromagnetic order of the localized moments and a spin-triplet state of the pair condensate (see discussion below).

3. Ferromagnetic manganites, spin-polarization, and half-metallicity

Magnetic and transport properties of manganites $R_{1-x}A_xMnO_3$, where trivalent cations R^{3+} are substituted by divalent ones A^{2+}, are discussed in detail in reviews [33–35]. Here we summarized the main ideas and statements.

Bulk samples. The initial compound $RMnO_3$ has a perovskite structure. It is electrically homogeneous due to the single valence of the Mn ion and below the Neel temperature $T_N \approx 130$ K exhibits an antiferromagnetic order. Compounds of the type $R_{1-x}A_xMnO_3$, where a divalent ion A^{2+} (= Ca, Sr, Ba, Pb, …) replaces the trivalent ion R^{3+}, are electrically inhomogeneous with a competition between different types of magnetic interactions among the Mn ions due to the random positions of ions Mn^{3+} and Mn^{4+} having different ionic radii, charges, and spins. When the concentration of the A^{2+} ions exceed ~1/8, the material undergoes a transition to a ferromagnetic state with a metallic type of conductivity. The Curie temperature of the ferromagnetic state depends significantly on the extent of substitution and the difference in the ionic radii of the A^{2+} and La^{3+} ions. The highest value of Curie temperature, close to 360 K, is attained in the compound $La_{5/8}Sr_{3/8}MnO_3$. The ferromagnetic–paramagnetic transition itself appears to be close to a second order phase transition and the behavior of the system is described by critical indices corresponding (or close) to a three-dimensional Heisenberg ferromagnet. (The specific realization of the metal-insulator transition in manganites with colossal magnetoresistance caused by inhomogeneities in the electronic and magnetic states of the manganites near the Curie temperature is reviewed in Ref. 35).

In terms of the traditional model proposed by Zener [36], the magnetic and transport properties of the substituted manganites are generated by the so-called "double-exchange" interaction. In brief, consider two cations Mn^{3+} and Mn^{4+} located at equivalent crystallographic positions and separated by an O^{2-} anion. The Mn^{4+} ion is in a t_{2g}^3 configuration and the Mn^{3+} ion is in a $t_{2g}^3 e_g^1$ configuration. Because of the large intra-atomic Hund coupling, the three electrons in the t_{2g} level form a localized spin $S = 3/2$. Due to the same Hund rule, the e_g electron on the Mn^{3+} ion has its spin aligned parallel to the localized spin of the ion. Since the positions of the Mn ions are equivalent, the Mn^{3+}–O^{2-}–Mn^{4+} and Mn^{4+}–O^{2-}–Mn^{3+} configurations are energetically equivalent, i.e., the ground state of the pair is degenerate. It is natural to expect a strong resonance coupling between the two configurations, which can be interpreted as a state of two Mn^{4+} cations with a generalized e_g-electron (or Mn^{3+} cations with a generalized hole). As an e_g-electron moves along the lattice it is energetically favorable that all the localized spins be parallel to one another, i.e., a ferromagnetic ordering of the localized spins minimizes the kinetic energy of the e_g-electrons. When the substitution degree is sufficiently high, the e_g-electrons form a ferromagnetic metallic state. As a result, in the ground state, all conducting electrons are spin-polarized in the direction of the spontaneous magnetic moment and there are no electrons with opposite spins. This type of metals is referred to as *half-metallic ferromagnet* (hmF), i.e., it is a metal for the majority spin and an insulator for the minority spin [37].

Experimental data on manganites with a perovskite structure, where the magnetic ions are ions of a single element with different valences, are in good qualitative and quantitative agreements with this model. For example, Bowen *et al.* present transport measurements of magnetic tunnel junctions with the manganite $La_{2/3}Sr_{1/3}MnO_3$ as the electrode material. The results obtained suggest that the electrode's current spin polarization is at least 95% [38].

Nanoparticles. A natural question arises whether the bulk characteristics of manganite are retained in nanosized samples. In Refs. 39–41 perovskite-type manganese oxide nanoparticles (NPs) with particle sizes of 15–30 nm and 100–200 nm were prepared and studied using ^{55}Mn nuclear magnetic resonance, superparamagnetic resonance, and magnetic measurements. The nuclear spin dynamics results provided direct evidence that the grain boundary of NPs is not sharp in the magnetic and electrical respects, but rather should be considered as a transfer region of several (~ two) monolayers with magnetic and structural orders different from the inner part of the grain. The cores of the NPs are magnetically homogeneous. The local structure of the outer shell is that of perovskites yet modified by vacancies, stress, disordering of atoms in perovskite cells and broken bonds on the surface. The Curie temperature, determined as the magnetization onset was close to that in a bulk crystalline sample of the same composition. Electrical transport properties support this physical picture. These mean that the particle's inner parts are magnetically identical to a bulk sample of the same composition, and in the inner part the strength of the double exchange interaction and the half-metallic conductivity are preserved.

4. Local triplet superconductivity of half-metallic manganites

Ferromagnetic order and singlet superconductivity are incompatible because the magnetic exchange field breaks apart the opposite-spin Cooper pairs. Equal-spin triplet Cooper pairs are immune to the exchange field and can propagate into ferromagnetic metals over the same long-distance as singlet pairs into normal metals. However, superconductors realizing a spin-triplet *p*-wave pairing are not common in nature; Sr_2RuO_4 being the only real candidate, so far. That is why artificial materials demonstrating equal-spin triplet superconductivity have attracted notable interest. Currently, this interest is motivated as condensed matter where the topological superconducting phase with specific quasiparticle excitations can be realized and as promising materials yielding novel technological applications.

Long-range proximity effects interpreted in terms of singlet-to-triplet pairing conversion have been found in various SC/ferromagnet (SCF) systems [42–52]. Among these systems, the half-metallic-based SC/F heterostructures, where the long-range proximity effect has been experimentally observed, have attracted especial attention [12–14, 48]. As was shown theoretically, for the SC/F systems, long-range proximity effect and singlet-to-triplet pairing conversion can be realized due to interfacial magnetic inhomogeneities. Eschrig *et al.* showed that when normal metal is half-metallic ferromagnet, even frequency pairing would be mostly of the *p*-wave symmetry [49].

As is known, at energies below the superconducting gap, the charge transport through a normal (N) nonmagnetic metal been in contact with a SC is possible only due to the specific two-particle process, called the Andreev reflection (AR) [50]. It consists in the fact that in the N metal, an incident electron above the Fermi energy E_F and an electron below E_F with the opposite spin are coupled together and transferred across the interface into the SC side, forming a singlet Cooper pair in the condensate. Simultaneously, an evanescent hole with opposite momentum and spin appears in the N metal. The point-contact AR spectroscopy [51, 52] is a direct and sensitive method of studying such local microscopic characteristics of a SC as the density of quasiparticle states, the superconducting gap value, the symmetry of a superconducting pairing, etc. Below we will use the results obtained by the point-contact technique in studies of a superconducting state and the symmetry of the superconducting pairing in *s* wave SC/hmF proximity coupled structures [15–19, 53, 54].

The superconducting proximity effect can induce new superconducting states in a contacted region. Anomalous superconductivity has been detected in point contacts (PCs) of half-metallic manganites (La,Sr)MnO_3 and (La,Ca)MnO_3 with an *s* wave SC, Pb or MgB_2 [16–19, 53, 54]. The study of the current-voltage (*I*–*V*) characteristics and of the dynamic conductance of PCs between the MgB_2:(La,Sr)MnO_3 *nanocomposite* with (3:1) volume ratio and different metallic needles (In, Ag, Nb, and $La_{0.65}Ca_{0.35}MnO_3$) has been performed and also supported new superconducting state in proximity-affected regions. The key findings are summarized in Fig. 1. The figure shows representative dynamic conductance spectra $dI/dV = G(V)$ of point contacts In, Ag, and Nb tips and the nanocomposite MgB_2:(La,Sr)MnO_3 sample measured at $T = 4.2$ K. At low voltages, conductance peaks corresponding to *three* superconducting gaps with energies $\Delta(\pi) = 2.0$–2.4 meV, $\Delta(\sigma) = 8.4$–11.7 meV, and $\Delta_{tr} = 19.8$–22.4 meV are clearly observed. (In the figure the position of the dI/dV minimum is denoted by Δ. For PCs with not too large lifetime-broadening effects, this value does not differ much from the proper energy gap [55].) Two of the gaps, $\Delta(\pi)$ and $\Delta(\sigma)$, were identified as MgB_2 gaps (to be precise, as ones originating from the $\Delta(\pi)$ and $\Delta(\sigma)$ gaps of MgB_2, respectively). The magnitude of the smallest

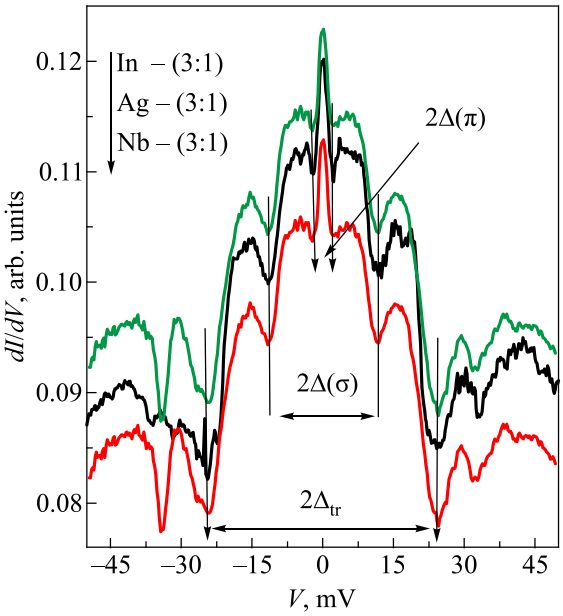

Fig. 1. (Color online) Point-contact Andreev reflection spectra of In, Ag, and Nb tips and MgB_2:$La_{0.67}Sr_{0.33}MnO_3$ (3:1) nanocomposite; $T = 4.2$ K. (Borrowed form Ref. 18).

$\Delta(\pi)$ gap remains in a range of the bulk MgB_2 gap [56]; the gap $\Delta(\sigma)$ was recognized as *enhanced* MgB_2 $\Delta(\sigma)$ gap. The third gap, Δ_{tr}, the authors [18] attributed to the intrinsic superconducting pairing in the (La,Sr)MnO_3 compound. The absolute value of Δ_{tr} is the same as those also detected in PCs of (La,Sr)MnO_3 and (La,Ca)MnO_3 with Pb or MgB_2 [16, 17, 53]. The magnitude of Δ_{tr} is more than *three times larger* than the largest "parents" $\Delta(\sigma) = 6.8$–7.1 meV MgB_2 gap [56]. Note that the PCs' resistivity varied by orders of magnitude, while the multiple-gap structure in the quasiparticle density of states, as well as the gap energy values, were robust features and reproduced in all PCs have been prepared.

In Fig. 2, the experimental temperature dependence of the energy gap $\Delta_{tr}(T)$ is shown [18]. For comparison, the conventional BCS gap temperature behavior is shown in the figure, too. From the BCS relation $\Delta(0) = 1.76\, k_B T_c$, the $\Delta_{tr}(0) = 19.8$–22.4 meV gap would lead to a superconducting state with $T_c \approx 120$ K. Yet, the energy gap $\Delta_{tr}(T)$ vanishes as the temperature increases towards $T_c \approx 39$ K of MgB_2. Evidently, the experimental behavior of $\Delta_{tr}(T)$ does not follow the BCS dependence. The temperature dependence of the largest gap detected, $\Delta_{tr}(T)$, directly proves that its emergence is not an "independent" property but is due to the superconducting state of MgB_2, i.e., due to the proximity effect.

These results are weighty arguments that proximity-induced superconducting transition in doped manganites follows the scenario of a "latent" high-T_c superconductivity in doped manganites. At low temperatures, incoherent superconducting fluctuations are essentially sustained in half-metallic manganites. Although the local gap amplitude is

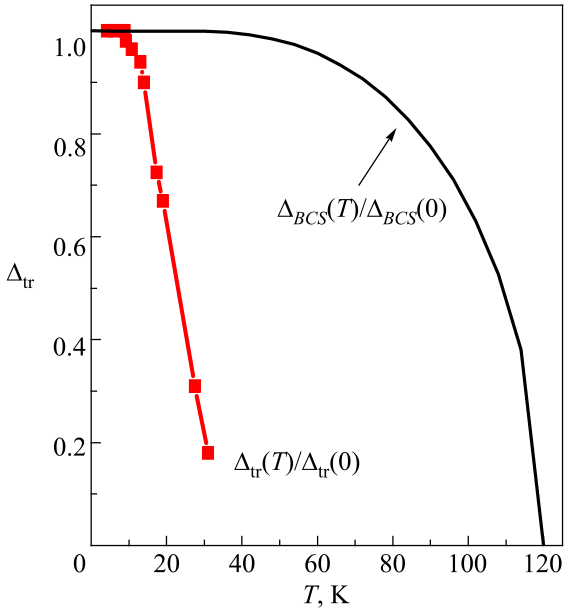

Fig. 2. (Color online) The experimental (square points) $\Delta_{tr}(T)$ gap temperature behavior (normalized to the zero-temperature gap) of the MgB_2:$La_{0.67}Sr_{0.33}MnO_3$ (3:1) nanocomposite and the BCS gap temperature dependence (black solid line). (Borrowed form Ref. 18).

large, there is no phase stiffness, and the system is incapable of displaying a long-range superconducting response. Nonetheless, a local phase rigidity (a local triplet pairing condensate) survives, and, in a proximity-affected region, the singlet SC establishes phase coherence of the *p* wave spin-triplet superconducting state of the manganites [16–19].

5. Bosonic scenario of local triplet superconductivity of half-metallic manganites

Let us make some suggestions concerning the mechanism of coupling spin-polarized conducting electrons in manganites and the origin of the quasiparticle gap Δ_{tr} whose magnitude cannot be explained in terms of the conventional proximity-effect theory.

In the context of manganite's half-metallic conductivity in the ferromagnetic state, a natural question arises about triplet superconductivity due to magnon coupling. The replacement of a phonon by a spin-wave should not lead to a drastic modification of superconducting properties. However, there is an important difference between these couplings [57]. Namely, spin-wave (magnon) carries a spin with the projection opposite to the ferromagnet magnetization direction and in the nonrelativistic approach, the projection of the total spin of both conducting and localized electrons is preserved. This means that if the magnon exchange results in equal-spin triplet pair states $\Delta_\uparrow$ or $\Delta_\downarrow$, neither $\Delta_\uparrow$ state nor $\Delta_\downarrow$ one can exist without each other since the magnon carries spin $|S| = 1$ and thus the attraction of two electrons with the *same* spins, +1/2 (or –1/2) due to spin-wave exchange is forbidden by the spin conservation law. As Bulaevskii, *et al.* showed [57], the spin-wave exchange mechanism leads to equal spin-triplet pairing but the resulting superconducting state is described by the two-component order parameter, $f^{tr}(r) = g_1(r)|\uparrow\uparrow> + g_2(r)|\downarrow\downarrow>$, and *excludes a singlet* $m = 0$ pairing, $f^{tr}_{\uparrow\downarrow}(r) = (|\uparrow\downarrow> + |\downarrow\uparrow>)$.

The conclusion above that the magnon exchange excludes a singlet pairing is important in the context of the experimental results [16–19]. Broken a spin-rotation symmetry at *s*-wave SC — half-metallic manganites interface leads to spin-flip processes at the interfaces. Its origin depends on the microscopic magnetic state at the interface, the character of local magnetic moments coupling with itinerant electrons, etc. (see, e.g., [14, 48] and references therein). Due to spin mixing at the interfaces, a spin-triplet ($S = 1$, $m = 0$) amplitude $f^{tr}_{\uparrow\downarrow}(r) = (|\uparrow\downarrow> + |\downarrow\uparrow>)$ is induced by the singlet component in the *s* wave SC, $f^{s}_{\uparrow\downarrow}(r) = (|\uparrow\downarrow - |\downarrow\uparrow)$, and extends from the interface for about the magnetic length $\xi_F = (D_F/2\pi H_{exc})^{1/2}$ into the manganites layer (here D_F is the diffusivity and H_{exc} stands for the exchange field in the half-metallic manganites, and we choose $\hbar = k_B = 1$). At the same time, triplet pairing correlations with equal spin pairs: $f^{tr}_{\uparrow\uparrow}(r) = |\uparrow\uparrow>$, $m = +1$ or $f^{tr}_{\downarrow\downarrow}(r) = |\downarrow\downarrow>$, $m = -1$, are also induced (due to spin-flip processes) in the half-metallic layer. These components decay on a "conventional" length scale $\xi_T = (D_F/2\pi T)^{1/2}$ which is much larger than ξ_F because in typical cases the exchange field H_{exc} is much larger than T_c. It is worthy to emphasis that only the $m = 0$ triplet component $f^{tr}_{\uparrow\downarrow}(r) = (|\uparrow\downarrow> + |\downarrow\uparrow>)$ is coupled via the spin-active boundary condition to the equal-spin $m = 1$ pairing amplitudes in the half-metal. The singlet component in the *s*-wave superconductor, $f^{s}_{\uparrow\downarrow}(r) = (|\uparrow\downarrow - |\downarrow\uparrow)$, being invariant under rotations around any quantization axis, cannot be directly involved in the creation of the triplet $m = \pm 1$ pairing amplitudes in the half-metal. Taking this into account, the observed *enhancement* of MgB_2 *even frequency singlet* Cooper pair coupling energy $\Delta(\sigma)$ means that in the manganite the $m = 0$ *even frequency triplet* component exists, i.e., the proximity induced superconducting state is described by the two-component order parameter, $f^{tr}(r) = g_1(r)|\uparrow\uparrow> + g_2(r)$ $(|\uparrow\downarrow> + |\downarrow\uparrow>)$. The $m = 0$ triplet component $f^{tr}_{\uparrow\downarrow}(r)$ is coupled via the boundary condition to the singlet pairing amplitude in the SC partner and, in this case, we deal with the "mutual" proximity effect. As well, this points out that the most realistic coupling mechanism of the *p*-wave triplet superconductivity in half-metallic manganites is that caused by the *phonon* exchange.

As already mentioned, one of the Cooper pairs fluctuation fingerprints is the so-called pseudo-gap [20–26], the reduction of the single-electron density of state near the Fermi level. At the Fermi level vicinity of manganites, a large pseudo-gap is observed [58–60]. This experimental fact supports the hypothesis that a noncoherent *p*-wave even-frequency spin-triplet superconducting condensate already exists in half-metallic manganites at low temperatures [16–19]. Being proximity coupled to a singlet SC,

the $m = 0$ triplet component in the manganite is coupled via the boundary condition to the singlet pairing amplitude in the SC partner. At the same time, the spin-active boundary leads to coupling of the $m = 0$ triplet component with an equal-spin, $m = 1$, pairing amplitude in a manganite. These couplings yield to a phase coherency of both the $m = 0$ and equal-spin $m = 1$ triplet Cooper pairs with a large quasiparticle gap $\Delta_{tr} > \Delta(\pi)$, $\Delta(\sigma)$. As an inverse effect, being proximity linked to the *s*-wave pairing amplitude, the $m = 0$ amplitude of the triplet superconducting state enhances the quasiparticle gap(s) in a singlet SC.

6. High-temperature topological superconductivity in superconductor–manganites nanostructured samples

At the actual stage of the search for topological quasiparticles in condensed matter, it is crucially desirable to identify (i) easy-to-fabricate systems possessing topological states and (ii) a way by which topologically protected excitations can be distinguished from spurious effects. Specifically, the realization of a topological superconducting phase and Majorana quasiparticles is of grand interest because of their novelty as well as their possible applications in quantum devices. Thereupon, a convincing proof and undoubted detection of Majorana quasiparticles are among the main challenges in the general trend.

There is a variety of proposals for transforming a conventional *s*-wave SC into topological states supporting Majorana fermion excitations. For instance, realizations of Majorana bound states are expected in semiconducting-superconducting hybrid nanostructures, where the interplay between intrinsic spin-orbit coupling, proximity induced superconductivity, and external magnetic field lead to the formation of zero-energy bound states [5–9, 61–71]. An isolated zero-energy topological bound state appears in a spin-less *p*-wave SC at the transition between strong- and weak-pairing phases. It is expected [63, 65–69] that one or more Majorana bound states can appear at the opposite ends of a quantum nanoparticle wire proximity coupled to an *s*-wave SC in the presence of an applied Zeeman field. Yet, while the time-reversal symmetry can be readily broken by a magnetic field, spin-orbit coupling is too weak to effectively break the spin-rotation symmetry and to drive the system into topologically nontrivial phase by this Kitaev scenario [72].

In Ref. 5 Choy, *et al.* proposed an alternative to Kitaev route to Majorana fermions in *s*-wave SCs that does not at all require materials with spin-orbit coupling and external Zeeman field. The authors considered a system formed by magnetic nanoparticles on a superconducting substrate. The magnetic moments are frozen, without any dynamics of their own. The nanoparticle's magnetic moment breaks time-reversal symmetry as well as spin-rotation symmetry, without the need for spin-orbit coupling in the SC. The superconducting substrate induces pairing energy in the nanoparticles so that the system's single-band Hamiltonian has the same form as Kitaev spinless *p*-wave superconducting chain [5]. The difference is that here the *p*-wave pairing is obtained from *s*-wave pairing due to the coupling of the electron spin to local magnetic moments (the proximity effect). In the nanoparticles wire, the transition into the topologically nontrivial superconducting phase is governed by the competition of two types of disorder: (i) variation in the orientation of the magnetic moments on nearby nanoparticles and (ii) disorder in the hopping energies that localizes the states. The zero-energy bound states in the proximity induced *p*-wave superconducting gap, having a nonzero magnetic moment, should behave as Majorana bound states [5].

In the context of Ref. 5 conclusions, we can suggest that nanostructures on the base of an *s*-wave SC substrate and hmF manganites nanoparticles are the most promising and accessible systems in which Majorana fermions can be generated. Indeed, all prerequisites listed in Ref. 5 can be realized in the heterostructures where magnetic nanoparticles are $(La_{1-x},R_x)MnO_3$, R = Ca, Sr, …, ones. Due to the ferromagnetic half-metallic state of the manganites, the needed *p*-wave superconductivity in the system is induced undoubtedly due to the proximity effect [16–19]. The key feature of these heterostructures is the magnitude of the proximity induced triplet superconducting gap Δ_{tr}, i.e., *the magnitude of the topological pairing gap* Δ_{top}. In manganite nanoparticles, this gap will be more than three times larger than the largest gap among *s*-wave SCs – the $\Delta(\sigma)$ gap MgB_2 [56]. Therefore, in our opinion, the manganite nanoparticles $(La_{1-x},R_x)MnO_3$ depositing on an *s*-wave SC are the most promising materials where *high-temperature topological superconducting states* can be realized. However, to our best knowledge, these systems have not yet been studied in detail, from this point of view.

7. Conclusion

In summary, systematic character and repeatability of the key experimental facts that have been detected by the point-contact Andreev reflection spectroscopy on the superconductor-half-metallic manganite heterostructures identify some general physical phenomena that have been observed in transport properties of proximity affected singlet superconductor-half-metallic manganite nanostructures. These experimental results point that superconductor–half-metallic manganite hybrids provide an experimental possibility to accomplish artificial materials where a topologically nontrivial superconducting state and Majorana fermions can be realized. The basic factor of these conclusions is a local (fluctuate) high-temperature triplet superconductivity in half-metallic manganites. Although the local gap amplitude is large, there is no phase stiffness, and the system is incapable of displaying a long-range superconducting state. Nonetheless, local phase rigidity survives, and being proxymity coupled to a superconductor, the long-range coherency is restored. The experimental evidence of the latent spin-triplet

superconductivity of half-metal manganites allows a design experimentally accessible way to overcoming the bottleneck of spin-triplet pairing induced in proximities structures of spin-singlet superconductors with time-reversal symmetry breaking counterparts and open a new framework in topological superconductivity. Further experimental and theoretical works are needed to prove (or disprove) this platform for engineering topological superconductors and Majorana fermions.

The author thanks M. A. Belogolovskii for reading the manuscript and fruitful discussions. The work has been partly supported by the NAS of Ukraine targeted fundamental research program "Promising basic research and innovative development of nanomaterials and nanotechnologies for industry, health, and agriculture" (Project No. 17/21-H).

———

1. J. Alicea, *Rep. Prog. Phys.* **75**, 076501 (2012).
2. C. W. J. Beenakker, *Annu. Rev. Condens. Matter Phys.* **4**, 113 (2013).
3. M. Sato and Y. Ando, *Rep. Prog. Phys.* **80**, 076501 (2017).
4. A. V. Balatsky, I. Vekhter, and J.-X. Zhu, *Rev. Mod. Phys.* **78**, 373 (2006).
5. T.-P. Choy, J. M. Edge, A. R. Akhmerov, and C. W. J. Beenakker, *Phys. Rev. B* **84**, 195442 (2011).
6. S. B. Chung, H.-J. Zhang, X.-L. Qi, and S.-Ch. Zhang, *Phys. Rev. B* **84**, 060510(R) (2011).
7. S. Nadj-Perge, I. K. Drozdov, B. A. Bernevig, and A. Yazdani, *Phys. Rev. B* **88**, 020407(R) (2013).
8. A. Gorczyca-Goraj, T. Domański, and M. M. Maśka, *Phys. Rev. B* **99**, 235430 (2019).
9. D. Crawford, E. Mascot, D. K. Morr, and S. Rachel, *Phys. Rev. B* **101**, 174510 (2020).
10. M. Kasai, T. Ohno, Y. Kanke, Y. Kozono, M. Hanazono, and Y. Sugita, *Jpn. J. Appl. Phys.* **29**, L2219 (1990).
11. M. Kasai, Y. Kanke, T. Ohno, and Y. Kozono, *J. Appl. Phys.* **72**, 5344 (1992).
12. Y. Kalcheim, T. Kirzhner, G. Koren, and O. Millo, *Phys. Rev. B* **83**, 064510 (2011).
13. C. Visani, Z. Sefrioui, J. Tornos, C. Leon, J. Briatico, M. Bibes, A. Barthélémy, J. Santamaría, and J. E. Villegas, *Nat. Phys.* **8**, 539 (2012).
14. M. Eschrig and T. Löfwander, *Nat. Phys.* **4**, 138 (2008).
15. A. I. D'yachenko, V. N. Krivoruchko, and V. Yu. Tarenkov, *Fiz. Nizk. Temp.* **32**, 1085 (2006) [*Low Temp. Phys.* **32**, 824 (2006)].
16. V. Krivoruchko and V. Tarenkov, *Phys. Rev. B* **75**, 214508 (2007).
17. V. Krivoruchko and V. Tarenkov, *Phys. Rev. B* **78**, 054522 (2008).
18. V. Krivoruchko and V. Tarenkov, *Phys. Rev. B* **86**, 104502 (2012).
19. V. Krivoruchko, A. D'yachenko, and V. Tarenkov, *Fiz. Nizk. Temp.* **40**, 1147 (2014) [*Low Temp. Phys.* **40**, 895 (2014)].
20. V. M. Loktev, R. M. Quick, and S. G. Sharapov, *Phys. Rep.* **349**, 1 (2001).
21. V. F. Gantmakher and V. T. Dolgolopov, *Usp. Fiz. Nauk* **180**, 3 (2010) [*Phys. Usp. Fiz. Nauk* **53**, 1 (2010)].
22. V. F. Gantmakher, *Fiz. Nizk. Temp.* **37**, 71 (2011) [*Low Temp. Phys.* **37**, 59 (2011)].
23. V. J. Emery and S. A. Kivelson, *Phys. Rev. Lett.* **74**, 3253 (1995).
24. E. Berg, D. Orgad, and S. A. Kivelson, *Phys. Rev. B* **78**, 094509 (2008).
25. M. Mondal, A. Kamlapure, M. Chand, G. Saraswat, S. Kumar, J. Jesudasan, L. Benfatto, V. Tripathi, and P. Raychaudhuri, *Phys. Rev. Lett.* **106**, 047001 (2011).
26. B. Sacépé, T. Dubouchet, C. Chapelier, M. Sanquer, M. Ovadia, D. Shahar, M. Feigel'man, and L. Ioffe, *Nature Phys.* **7**, 239 (2011).
27. J. Mitra, A. K. Raychaudhuri, Ya. M. Mukovskii, and D. Shulyatev, *Phys. Rev. B* **68**, 134428 (2003).
28. T. Saitoh, D. S. Dessau, Y. Moritomo, and T. Kimura, *Phys. Rev. B* **62**, 1039 (2000).
29. V. Yu. Tarenkov, A. I. D'yachenko, and V. N. Krivoruchko, *Zh. Éksp. Teor. Fiz.* **120**, 205 (2001) [*JETP* **93**, 180 (2001)].
30. M. Edwards, *Adv. Phys.* **51**, 1259 (2002).
31. I. Iguchi, T. Yamaguchi, and A. Sugimoto, *Nature* **412**, 420 (2001).
32. J. L. González and E. V. L. de Mello, *Phys. Rev. B* **69**, 134510 (2004).
33. E. Dagotto, T. Hotta, and A. Moreo, *Phys. Rep.* **344**, 1 (2001).
34. M. Ziese. *Rep. Prog. Phys.* **65**, 143 (2002).
35. V. N. Krivoruchko, *Fiz. Nizk. Temp.* **40**, 756 (2014) [*Low Temp. Phys.* **40**, 586 (2014)].
36. C. Zener, *Phys. Rev.* **22**, 403 (1951).
37. R. A. de Groot, F. M. Mueller, P. G. van Engen, and K. H. J. Buschow, *Phys. Rev. Lett.* **50**, 2024 (1983).
38. M. Bowen, M. Bibes, A. Barthélémy, J.-P. Contour, A. Anane, Y. Lemaître, and A. Fert, *Appl. Phys. Lett.* **82**, 233 (2003).
39. M. M. Savosta, V. N. Krivoruchko, I. A. Danilenko, V. Yu. Tarenkov, T. E. Konstantinova, A. V. Borodin, and V. N. Varyukhin, *Phys. Rev. B* **69**, 024413 (2004).
40. V. Krivoruchko, T. Konstantinova, A. Mazur, A. Prokhorov, and V. Varyukhin, *J. Magn. Magn. Mater.* **300**, e122 (2006).
41. A. N. Ulyanov, D. S. Yang, A. S. Mazur, V. N. Krivoruchko, G. G. Levchenko, I. A. Danilenko, and T. E. Konstantinova, *J. Appl. Phys.* **109**, 123928 (2011).
42. F. S. Bergeret, A. F. Volkov, and K. B. Efetov, *Phys. Rev. Lett.* **86**, 4096 (2001).
43. R. S. Keizer, S. T. B. Goennenwein, T. M. Klapwijk, G. Miao, G. Xiao, and A. Gupta, *Nature (London)* **439**, 825 (2006).
44. M. S. Anwar, F. Czeschka, M. Hesselberth, M. Porcu, and J. Aarts, *Phys. Rev. B* **82**, 100501 (2010).
45. T. S. Khaire, M. A. Khasawneh,W. P. Pratt, Jr., and N. O. Birge, *Phys. Rev. Lett.* **104**, 137002 (2010).
46. D. Sprungmann, K. Westerholt, H. Zabel, M. Weides, and H. Kohlstedt, *Phys. Rev. B* **82**, 060505 (2010).
47. J. W. A. Robinson, J. D. S. Witt, and M. G. Blamire, *Science* **329**, 59 (2010).
48. M. Eschrig, *Phys. Today* **64**, 43 (2011).
49. M. Eschrig, J. Kopu, J. C. Cuevas, and G. Schön, *Phys. Rev. Lett.* **90**, 137003 (2003).

50. A. F. Andreev, *Zh. Éksp. Teor. Fiz.* **46**, 1823 (1964) [*Sov. Phys. JETP* **19**, 1228 (1964)].
51. Y. G. Naidyuk and I. K. Yanson, *Point-Contact Spectroscopy*, Springer (2005).
52. M. Eschrig, *Phil. Trans. R. Soc. A* **376**, 20150149 (2018).
53. A. I. D'yachenko, V. A. D'yachenko, V. Yu. Tarenkov, and V. N. Krivoruchko, *Fiz. Tverd. Tela* **48**, 407 (2006) [*Phys. Solid State* **48**, 432 (2006)].
54. V. N. Krivoruchko, A. I. Dyachenko, V. Y. Tarenkov, *Fiz. Nizk. Temp*. **39**, 276 (2013) [*Low Temp. Phys.* **39**, 211 (2013)].
55. R. C. Dynes, V. Narayanamurti, and J. P. Garno, *Phys. Rev. Lett.* **41**, 1509 (1978).
56. X. X. Xi, *Rep. Prog. Phys*. **71**, 116501 (2008).
57. L. Bulaevskii, R. Eneias, and A. Ferraz, *Phys. Rev. B* **99**, 064506 (2019).
58. J. Mitra, A. K. Raychaudhuri, Ya. M. Mukovskii, and D. Shulyatev, *Phys. Rev. B* **68**, 134428 (2003).
59. T. Saitoh, D. S. Dessau, Y. Moritomo, and T. Kimura, *Phys. Rev. B* **62**, 1039 (2000).
60. M. Edwards, *Adv. Phys*. **51**, 1259 (2002).
61. J. D. Sau, S. Tewari, R. M. Lutchyn, T. D. Stanescu, and S. das Sarma, *Phys. Rev. B* **82**, 214509 (2010).
62. T.-P. Choy, J. M. Edge, A. R. Akhmerov, and C. W. J. Beenakker, *Phys. Rev. B* **84**, 195442 (2011).
63. M. Wimmer, A. R. Akhmerov, J. P. Dahlhaus, and C. W. J. Beenakker, *New J. Phys.* **13**, 053016 (2011).
64. S. Nakosai, Y.Tanaka, and N. Nagaosa, *Phys. Rev. B* **88**, 180503(R) (2013).
65. V. Mourik, K. Zuo, S. M. Frolov, S. R. Plissard, E. P. A. M. Bakkers, and L. P. Kouwenhoven, *Science* **336**, 1003 (2012).
66. A. Das, Y. Ronen, Y. Most, Y. Oreg, M. Heiblum, and H. Shtrikman, *Nat. Phys.* **8**, 887 (2012).
67. M. T. Deng, C. L. Yu, G. Y. Huang, M. Larsson, P. Caroff, and H. Q. Xu, *Nano Lett.* **12**, 6414 (2012).
68. J. Liu, A. C. Potter, K. T. Law, and P. A. Lee, *Phys. Rev. Lett.* **109**, 267002 (2012).
69. D. I. Pikulin, J. P. Dahlhaus, M. Wimmer, H. Schomerus, and C. W. J. Beenakker, *New J. Phys.* **14**, 125011 (2012).
70. D. Bagrets and A. Altland, *Phys. Rev. Lett.* **109**, 227005 (2012).
71. C.-X. Liu, J. D. Sau, T. D. Stanescu, and S. das Sarma. *Phys. Rev. B* **96**, 075161 (2017).
72. A. Yu. Kitaev, *Phys. Usp*. **44**, 131 (2001).

Локальна спін-триплетна надпровідність в напівметалевих манганітах: перспективна платформа для високотемпературної топологічної надпровідності

V. N. Krivoruchko

Топологічні матеріали та їх особливі властивості зараз перебувають у центрі уваги сучасних експериментальних та теоретичних досліджень. Перспективними матеріалами для реалізації топологічної надпровідної фази є матеріали зі спін-триплетним надпровідним станом. Проте природні надпровідники, що реалізують спін-триплетне *p*-хвильове спарювання, є винятком. Експериментально доступним способом подолання цього обмеження є спін-триплетне спарювання, індуковане в близькісних структурах спін-синглетних надпровідників із складовими компонентами, що порушують симетрією щодо інверсії часу. Обговорено можливість створення таких матеріалів на основі наноструктур надпровідник–напівметалевий манганіт. Унікальним багатообіцяючим фактором цих близькісних гібридних структур є високотемпературна локальна триплетна надпровідність у напівметалевих манганітах. Наведено експериментальні докази прихованого спін-триплетного спарювання в напівметалевих манганітах та обговорено умови, що сприяють топологічному надпровідному стану наноструктур на їх основі.

Ключові слова: напівметалеві манганіти, локальні надпровідні куперівські пари, топологічна надпровідність, напівметалеві-надпровідникові гетероструктури.